

Chapter 2

Mathematical Modeling

Abstract This chapter presents a detailed mathematical analysis of PTCs. It is divided into three sections: tracking of the Sun, optical analysis and thermal analysis. The first section is an overview of equations and relationships used in solar geometry to determine the position of the Sun and, hence, the slope and the angle of incidence that in each instant must be assumed by a PTC to correctly follow the Sun. Since PTCs usually have one degree of freedom, correlations valid for east-west and north-south axis with continuous adjustment are discussed. The optical analysis starts by introducing the concentration ratio and continues presenting a thorough description of the geometry of a PTC. Optical errors and geometrical effects are also presented. Then, the optical analysis is concluded by taking into account the optical properties of the materials generally adopted in PTCs: the mirror, the cover and the absorber. The last section involves the thermal analysis of a PTC, i.e. the energy balance of the receiver. Each heat flux is described in detail, in order to determine the thermal efficiency of a PTC.

Keywords Tracking · Solar angles · Optical errors · Concentration ratio · Energy balance

2.1 Tracking of the Sun

This section intends to supply the reader with the essential equations to calculate the position of the Sun. Specific equations to be used with PTCs will be also given.

2.1.1 Solar Time

With the term *solar time*, we intend the time based on the apparent angular motion of the Sun across the sky. The time the Sun crosses the meridian of the observer is called *solar noon*. Solar time does not coincide with local clock time (LCT); it is necessary to convert standard time to solar time by applying two corrections [1]:

1. the first correction is for the difference in longitude between the observer's meridian and the meridian on which the local standard time is based;
2. the second correction derives from the equation of time, which accounts for the perturbations in the Earth's rate of rotation that affects the time the Sun crosses the observer's meridian.

The difference expressed in minutes between solar time and standard time is [1]:

$$\text{Solar Time} - \text{Standard Time} = 4 (L_{\text{st}} - L_{\text{loc}}) + E \quad (2.1)$$

where L_{st} is the standard meridian for the local time zone and L_{loc} is the longitude of the site (longitudes are in degrees west). The symbol E denotes the equation of time, expressed in minutes [1]:

$$E = 229.2 (0.000075 + 0.001868 \cos B - 0.032077 \sin B - 0.014615 \cos 2B - 0.04089 \sin 2B) \quad (2.2)$$

where

$$B = (n - 1) \frac{360}{365} \quad (2.3)$$

In Eq. (2.3), n is the n th day of the year. Note that Eq. (2.2) and all the equations in the following use degrees and not radians. Time is assumed to be solar time unless indication is given otherwise.

2.1.2 Solar Angles

The Sun's position with respect to a plane of any particular orientation to the Earth at any time can be described in terms of several angles, reported in Fig. 2.1. The angles and their sign conventions are as follows [1].

- Latitude (ϕ): it is the angular location of a terrestrial site with reference to the Equator. It is north positive: $-90^\circ < \phi < 90^\circ$.
- Declination (δ): it is the angular position of the Sun at solar noon with respect to the plane of the Equator. It is north positive: $-23.45^\circ < \delta < 23.45^\circ$. The declination can be found with an error less than 0.035° with the following equation [1]:

$$\delta = (180/\pi)(0.006918 - 0.399912 \cos B + 0.070257 \sin B - 0.006758 \cos 2B + 0.000907 \sin 2B - 0.002697 \cos 3B + 0.00148 \sin 3B) \quad (2.4)$$

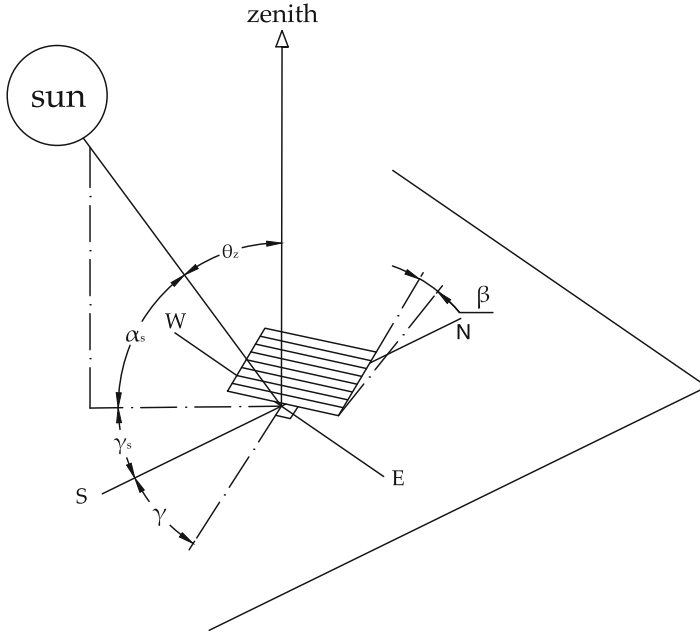


Fig. 2.1 Solar angles for a tilted surface. Adapted from [1]

where B was defined in Eq. (2.3).

- Slope (β): it is the angle between the plane of a surface and the horizontal. If it is greater than 90° , the surface has a downward-facing component: $0^\circ < \beta < 180^\circ$.
- Surface azimuth angle (γ): it is the deviation of the projection on a horizontal plane of the normal to the surface from the local meridian. It is zero due south, east negative and west positive: $-180^\circ < \gamma < 180^\circ$.
- Hour angle (ω): it is the angular displacement of the Sun east or west of the local meridian due to rotation of the Earth on its axis at 15° per hour. It is negative in the morning and positive in the afternoon.
- Angle of incidence (θ): it is the angle between the beam radiation on a surface and the normal to that surface. The angle of incidence is related to the above mentioned angles through the expression:

$$\begin{aligned} \cos \theta = & \sin \delta \sin \phi \cos \beta - \sin \delta \cos \phi \sin \beta \cos \gamma \\ & + \cos \delta \cos \phi \cos \beta \cos \omega + \cos \delta \sin \beta \sin \gamma \sin \omega \\ & + \cos \delta \sin \phi \sin \beta \cos \gamma \cos \omega \end{aligned} \quad (2.5)$$

The angle of incidence may exceed 90° , meaning that the Sun is behind the surface. Equation (2.5) implies that the hour angle is between sunrise and sunset.

- Zenith angle (θ_z): it is the angle between the vertical and the line of the Sun. If the surface is horizontal ($\beta = 0$), θ_z corresponds to the angle of incidence and

Eq. (2.5) becomes:

$$\cos \theta_z = \sin \delta \sin \phi + \cos \delta \cos \phi \cos \omega \quad (2.6)$$

- Solar altitude angle (α_s): it is the angle between the horizontal plane and the beam radiation. It is the complementary angle of the zenith.
- Solar azimuth angle (γ_s): it is the angular displacement from south of the projection of the line of the Sun on the horizontal plane. Displacements east of south are negative and west of the south are positive. The solar azimuth angle can be found with:

$$\gamma_s = \text{sgn}(\omega) \left| \cos^{-1} \left(\frac{\cos \theta_z \sin \phi - \sin \delta}{\sin \theta_z \cos \phi} \right) \right| \quad (2.7)$$

where the sign function is equal to +1 if ω is positive and to -1 if ω is negative.

2.1.3 Angles for Tracking Surfaces

Solar collectors such as PTCs track the Sun by moving in prescribed ways to minimize the angle of incidence of beam radiation on their surface and therefore maximize the incident direct radiation. In particular, PTCs can rotate about their axis that could have any orientation but in practice is usually horizontal east-west or horizontal north-south.

For a plane rotated about a horizontal east-west axis with continuous adjustment to minimize the angle of incidence [1]:

$$\cos \theta = \sqrt{1 - \cos^2 \delta \sin^2 \omega} \quad (2.8)$$

The slope of the surface can be calculated from:

$$\tan \beta = \tan \theta_z |\cos \gamma_s| \quad (2.9)$$

If the solar azimuth angle passes through $\pm 90^\circ$, the surface azimuth angle of orientation will change between 0° and 180° ; otherwise:

$$\gamma = \begin{cases} 0^\circ, & \text{if } |\gamma_s| < 90^\circ \\ 180^\circ, & \text{if } |\gamma_s| \geq 90^\circ \end{cases} \quad (2.10)$$

The shadowing effects of this arrangement are minimal; the principal shadowing is caused when the collector is tipped to a maximum degree south ($\delta = 23.5^\circ$) at winter solstice. In this case, the Sun casts a shadow toward the collector at the north. This configuration has the advantage to approximate the full tracking in summer;

however, the winter performance is seriously depressed relative to the summer one [2].

For a plane rotated about a horizontal north-south axis with continuous adjustment to minimize the angle of incidence [1]:

$$\cos \theta = \sqrt{\cos^2 \theta_z + \cos^2 \delta \sin^2 \omega} \quad (2.11)$$

The slope is:

$$\tan \beta = \tan \theta_z |\cos (\gamma - \gamma_s)| \quad (2.12)$$

In this arrangement, γ will be 90° or -90° depending on the sign of γ_s :

$$\gamma = \begin{cases} 90^\circ, & \text{if } \gamma_s > 0^\circ \\ -90^\circ, & \text{if } \gamma_s \leq 0^\circ \end{cases} \quad (2.13)$$

The greatest advantage of this arrangement is that very small shadowing effects are encountered when more than one collector is used. These occur only at the first and last hours of the day [2].

2.1.4 Beam Radiation on Tilted Surfaces

According to the instrument used to measure solar radiation, different relationships should be considered to identify the beam radiation which falls on a tilted surface.

Pyrheliometers are instruments able to measure the normal beam radiation, G_{bn} . Therefore, if G_{bn} measurements are available, the beam radiation on a tilted surface is (see Fig. 2.2):

$$G_{bt} = G_{bn} \cos \theta \quad (2.14)$$

On the other hand, pyranometers measure global (i.e., direct and diffuse) solar radiation referred to the horizontal plane, G . The same quantity is generally considered in estimates of solar radiation given by empirical equations. If we only consider the direct fraction G_b , from Fig. 2.2 we obtain that:

$$G_{bt} = G_{bn} \cos \theta = G_b \frac{\cos \theta}{\cos \theta_z} \quad (2.15)$$

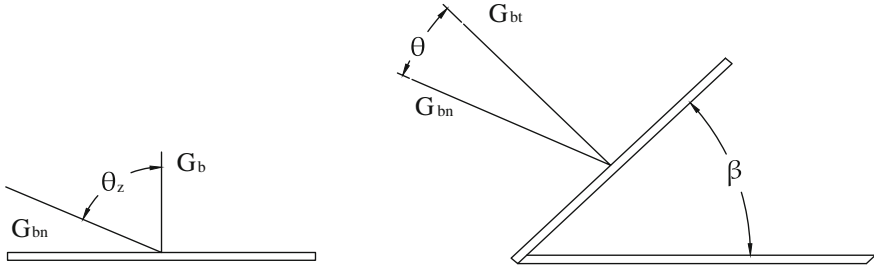


Fig. 2.2 Beam radiation on horizontal and tilted surfaces. Adapted from [1]

2.2 Optical Analysis

The optical analysis quantifies the amount of solar energy that actually reaches a PTC receiver. In the following sections, the parameters that influence a PTC optical efficiency will be analyzed.

2.2.1 Concentration Ratio

In PTCs, the concentration of solar radiation is achieved by reflecting the solar flux incident on the concentrator of aperture area A_a onto the receiver of area A_r . The concentration ratio, C , is referred to as the ratio of the aperture area to that of the receiver:

$$C = \frac{A_a}{A_r} \quad (2.16)$$

Generally, the higher the temperature at which energy is to be delivered, the higher should be the concentration ratio. This ratio has also an upper limit that depends on the second law of thermodynamics. Since PTCs are two-dimensional concentrating collectors, it is possible to demonstrate that the maximum achievable concentration ratio is [3]:

$$C_{\max} = \frac{1}{\sin \theta_m} \quad (2.17)$$

where θ_m is the acceptance half-angle the Sun subtends as seen from the Earth. For tracking collectors, θ_m is limited by the size of the Sun's disk, small-scale errors, irregularities of the reflector surface and tracking errors [2]. For a perfect PTC, C_{\max} depends only on the Sun's disk. In this case, the half-acceptance angle is 0.267° and we get:

$$C_{\max} \simeq 215 \quad (2.18)$$

The equation of the parabola can be integrated from 0 to $W_a/2$ (or from 0 to ϕ_r) to find its arc length:

$$L_p = \frac{f}{2} \left[\tan \frac{\phi_r}{2} \sec \frac{\phi_r}{2} + \ln \left(\tan \frac{\phi_r}{2} + \sec \frac{\phi_r}{2} \right) \right] \quad (2.23)$$

For specular reflectors of perfect alignment, the minimum size of the receiver of diameter D necessary to intercept all the reflected radiation is:

$$D = 2r_r \sin \theta_m \quad (2.24)$$

The proper value of the half-acceptance angle θ_m used in Eq. (2.24) depends on the accuracy of the tracking mechanism and the irregularities of the reflector surface. The smaller these two effects, the closer is θ_m to the Sun's disk angle, resulting in a smaller image and higher concentration. In Fig. 2.3, the incident beam of solar radiation is a cone with an angular width of 0.53° (a half-angle θ_m of 0.267°); it leaves the concentrator at the same angle. This situation occurs only with a perfect PTC. With a real PTC, the half-acceptance angle should be increased to include the presence of errors [2]. All these are accounted for by the intercept factor, which will be discussed in Sect. 2.2.3.

For a tubular receiver of the same length of the reflector, the concentration ratio is:

$$C = \frac{W_a}{\pi D} \quad (2.25)$$

Substituting Eqs. (2.22) and (2.24) into Eq. (2.25):

$$C = \frac{\sin \phi_r}{\pi \sin \theta_m} \quad (2.26)$$

C is maximum when $\sin \phi_r = 1$ (i.e., when $\phi_r = 90^\circ$). Therefore, Eq. (2.26) becomes:

$$C_{\max} = \frac{1}{\pi \sin \theta_m} \quad (2.27)$$

The difference between this equation and Eq. (2.17) is that the former applies to a PTC with a circular receiver, while the latter refers to the idealized case. In comparison with Eq. (2.18), and using the same half-acceptance angle of 0.267° , the maximum concentration ratio is $C_{\max} = 1/(\pi \sin 0.267^\circ) = 68.3$.

Finally, it can be demonstrated that, with $\phi_r = 90^\circ$, the mean focus-to-reflector distance and the reflected beam are minimized, so that the slope and tracking errors are less pronounced [4]. The collector's surface area, however, decreases as the rim angle decreases. Thus, there is a temptation to use smaller rim angles because the reduction in optical efficiency is small in comparison with the saving in reflective material cost [2].

2.2.3 Optical Errors

The upper limit to the concentration ratio which can be achieved by a PTC is set by the Sun's width, as seen in Sect. 2.2.1. However, in practical use, the concentration ratio is degraded below to this upper limit due to several factors:

- apparent changes in Sun's width and incidence angle effects;
- physical properties of the materials used in the construction;
- imperfections that may result from manufacture and/or assembly, imperfect tracking of the Sun, and poor operating procedures.

A depth study of all potential errors in PTCs was presented by Guven and Bannerot [5]. Errors can be divided into two groups: random errors and non-random errors (Fig. 2.4). Random errors are defined as truly random natural errors and, therefore, can be represented by normal distributions with mean equal to zero. They are treated statistically and are the origin of spreading of the reflected energy distribution. Random errors are:

- scattering effects associated with the optical material used in the reflector;
- scattering effects caused by random slope errors (e.g., waviness of the reflector due to distortions occurred during manufacturing and/or assembly);
- misalignment of the PTC with the Sun due to random tracking errors (which last only a very short period of time).

These errors can be modeled statistically by introducing a total reflected energy distribution standard deviation at normal incidence, $\sigma_{\text{tot},n}$, which is given by:

$$\sigma_{\text{tot},n} = \sqrt{\sigma_{\text{sun},n}^2 + \sigma_{\text{mirror},n}^2 + 4\sigma_{\text{slope},n}^2} \quad (2.28)$$

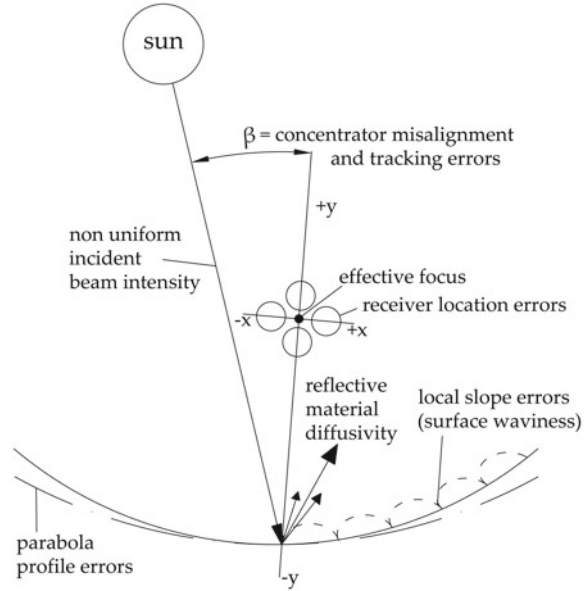
In this equation:

- $\sigma_{\text{sun},n}$ is the energy distribution standard deviation of the Sun's rays at normal incidence and solar noon;
- $\sigma_{\text{mirror},n}$ is the standard deviation of the distribution of diffusivity of the reflective material at normal incidence;
- $\sigma_{\text{slope},n}$ is the standard deviation of the distribution of local slope errors at normal incidence.

Non-random errors have a single deterministic value and can be related directly to anticipated errors in manufacture/assembly and/or in operation. In general, these errors will cause the central ray of the reflected energy distribution to shift from the design direction. Non-random errors can be classified as:

- Reflector profile errors (e.g., due to deflection or severe waviness of the reflector surface) which cause a permanent change in the location of the focus of the reflector, thus preventing the reflected radiation to reach the receiver. They can be quantified with the distance between the actual and ideal focus measured along the optical axis of the reflector.

Fig. 2.4 Optical errors in a PTC. Adapted from [5]



- Misalignment of the trough with the Sun (e.g., due to a constant tracking error) so that the position of the focus is shifted from the ideal focus and the central ray of the reflected beam can miss the receiver. The distance between the ideal focus of the concentrator and the center of the receiver can be used to quantify them.
- Misalignment of the receiver with the effective focus of the concentrator, that causes the central ray to miss the receiver. This quantity can be evaluated by defining an angle between the central solar ray and the normal to the concentrator aperture plane, β , as shown in Fig. 2.4.

Güven and Bannerot [5] showed that the receiver mislocation along the optical axis (y axis) degrades the optical performances more than the mislocation along the x axis (Fig. 2.4). Thus, the receiver mislocation along the optical axis, $(d_r)_y$, can be chosen to represent the non-random receiver location errors. Since the reflector profile errors and the receiver mislocation along y axis bring about the same effect, the parameter $(d_r)_y$ can account for both. Therefore, only two independent variables, $(d_r)_y$ and β , are sufficient to model non-random errors.

In summary, there are three error parameters that characterize optical errors: one random error, described by $\sigma_{\text{tot},n}$, and two non-random errors, described by $(d_r)_y$ and β , respectively. To quantify all the errors with a single parameter, the intercept factor is introduced. This is referred to as the fraction of reflected radiation that is incident on the absorbing surface of the receiver and it is a function of both random and non-random errors as well as the geometry of the collector:

$$\gamma = \gamma(\phi_r, C, D, \sigma_{\text{tot},n}, (d_r)_y, \beta) \quad (2.29)$$

Random and non-random errors can be combined with the geometrical parameters of the PTC to conduct an analysis valid for all PTC geometries [5]. The expression of γ derived by Guven and Bannerot [5] is:

$$\begin{aligned} \gamma = & \frac{1 + \cos \phi_r}{2 \sin \phi_r} \\ & \times \int_0^{\phi_r} \left\{ \operatorname{erf} \left(\frac{\sin \phi_r (1 + \cos \phi) (1 - 2d^* \sin \phi) - \pi \beta^* (1 + \cos \phi_r)}{\sqrt{2} \pi \sigma^* (1 + \cos \phi_r)} \right) \right. \\ & \quad \left. - \operatorname{erf} \left(- \frac{\sin \phi_r (1 + \cos \phi) (1 + 2d^* \sin \phi) + \pi \beta^* (1 + \cos \phi_r)}{\sqrt{2} \pi \sigma^* (1 + \cos \phi_r)} \right) \right\} \\ & \times \frac{d\phi}{1 + \cos \phi} \end{aligned} \quad (2.30)$$

where

- $\sigma^* = \sigma_{\text{tot},n}$ C is the universal random error parameter;
- $d^* = (d_r)_y/D$ is the universal non-random error parameter due to receiver mislocation and reflector profile errors;
- $\beta^* = \beta C$ is the universal non-random error due to angular errors.

Equation (2.29) can be therefore simplified as:

$$\gamma = \gamma (\phi_r, \sigma^*, d^*, \beta^*) \quad (2.31)$$

2.2.4 Geometrical Effects

Several abnormal incidence factors have the effect of reducing the optical performances of a PTC. These factors are:

- end effects;
- shading by integral bulkheads;
- intra-array shading.

Jeter et al. [6] presented a technique which ascribes to these effects the purely geometrical result of reducing the effective aperture of the concentrator.

During off-normal operation of a PTC, some of the rays reflected from near the end of the concentrator cannot reach the receiver. This loss of effective aperture is called end effect. PTCs can exhibit end effects since the receiver is usually terminated near the same cross-section plane as in the concentrator. The effective area lost to end effects is represented by the ruled region in Fig. 2.5 and is equal to [6]:

$$A_i = f w \tan \theta \left(1 + \frac{w^2}{48f^2} \right) \quad (2.32)$$

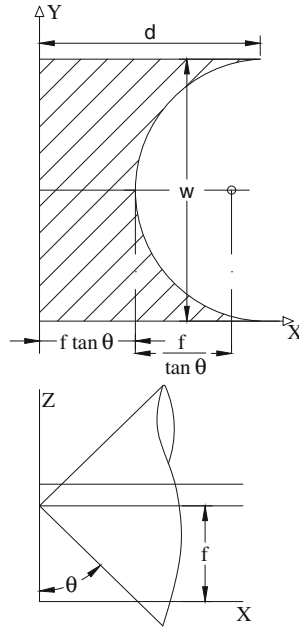


Fig. 2.5 Ineffective aperture area due to end effects. Adapted from [6]

where f is the focal distance, w is the parabola width and θ is the angle of incidence.

It is possible to reduce end effects by employing a receiver longer than the trough. If this solution is adopted, two cases must be considered, as Fig. 2.6 shows. If $S < A$ (Fig. 2.6a), the ineffective area is:

$$A_{i,1} = A_i - Sw \quad (2.33)$$

where S is the distance between the receiver rim and the concentrator rim. Instead, if $A < S < d$ (Fig. 2.6b), it can be demonstrated that the ineffective area is given by:

$$A_{i,2} = A_i + (Sw' - A'_i) - Sw \quad (2.34)$$

Clearly, if $S > d$, the ineffective area is equal to zero.

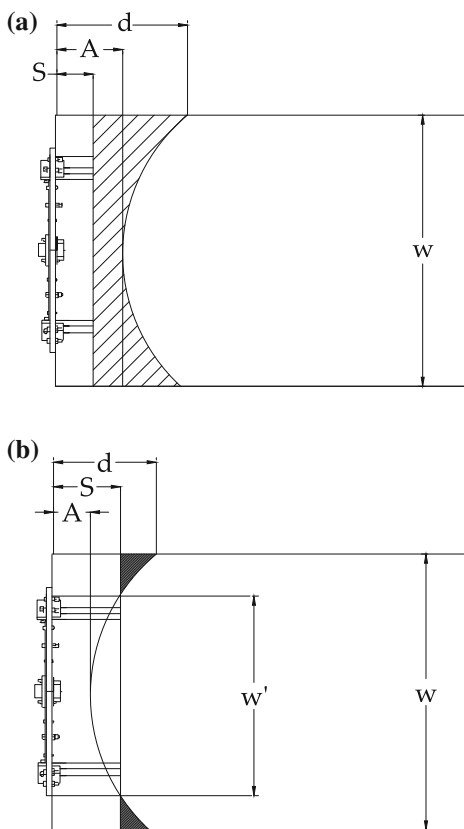
Combining the end effects with the shading produced by the receiver, the ratio of ineffective area to the whole aperture area is:

$$A_f = \frac{A_i + D_{ao}L_c}{A_a} \quad (2.35)$$

where D_{ao} is the cover outer diameter and L_c is the length of the concentrator. Thus, the effective aperture area is:

$$A_{ae} = A_a(1 - A_f) \quad (2.36)$$

Fig. 2.6 End effects when the receiver extends beyond the trough. **a** $S < A$.
b $A < S < d$



2.2.5 Optical Properties of Materials

The following sections present equations to calculate the optical properties of the materials adopted in a PTC, in particular the absorptance of the absorber and the transmittance of the glass cover.

2.2.5.1 Specular Reflectance of the Mirror

PTCs require the use of reflecting materials such to direct the beam radiation onto the receiver. Therefore, surfaces of high specular reflectance for radiation in the solar spectrum are required. Specular surfaces are usually metals or metallic coatings on smooth substrates. The specular reflectivity of such surfaces is a function of the quality of the substrate and the plating.

Specular reflectance generally depends on wavelength, so monochromatic reflectances should be integrated for the particular spectral distribution of incident beam radiation. Typical values of specular reflectance of surfaces for solar radiation are greater than 0.90.

2.2.5.2 Glass Cover

The transmittance of the glass cover of a PTC can be obtained with adequate accuracy by considering reflection and absorption separately, and is given by the product form:

$$\tau \simeq \tau_r \tau_a \quad (2.37)$$

where τ_r is the transmittance obtained by considering only reflection losses and τ_a is the transmittance obtained by considering only absorption losses.

The transmittance τ_r can be evaluated from:

$$\tau_r = \frac{1}{2} \left(\frac{1 - r_{\perp}}{1 + r_{\perp}} + \frac{1 - r_{\parallel}}{1 + r_{\parallel}} \right) \quad (2.38)$$

where r_{\perp} and r_{\parallel} are, respectively, the perpendicular and parallel components of the unpolarized radiation. Those components are given by the Fresnel's equations:

$$r_{\perp} = \frac{\sin^2(\theta_2 - \theta_1)}{\sin^2(\theta_2 + \theta_1)} \quad (2.39)$$

$$r_{\parallel} = \frac{\tan^2(\theta_2 - \theta_1)}{\tan^2(\theta_2 + \theta_1)} \quad (2.40)$$

In Fresnel's equations, θ_1 is the angle of incidence and θ_2 is the angle of refraction, as depicted in Fig. 2.7. The two angles are related by the Snell's law:

$$\frac{\sin \theta_1}{\sin \theta_2} = \frac{n_2}{n_1} \quad (2.41)$$

where n_1 and n_2 are the refraction indices of the two media forming the interface. Typical values of the refraction index are 1 for air and 1.526 for glass.

The absorption of radiation in a partially transparent medium is described by the Bouguer's law:

$$\tau_a = \exp \left(-\frac{Kt}{\cos \theta_2} \right) \quad (2.42)$$

where K is the extinction coefficient, which is assumed to be a constant in the solar spectrum, and t is the thickness of the glass cover. For glass, the value of K can vary from 4 m^{-1} (high-quality glass) to approximately 32 m^{-1} (low-quality glass).

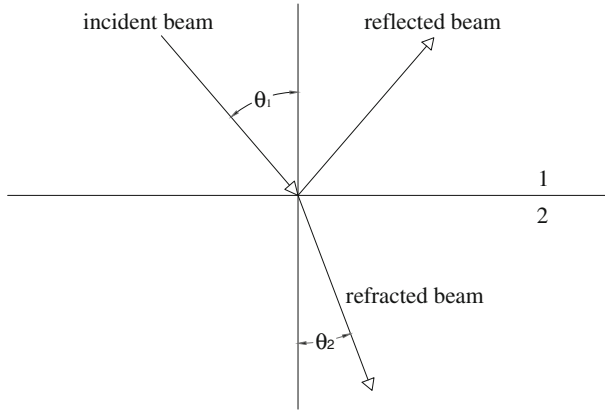


Fig. 2.7 Reflection and refraction at the interface of two media

The absorptance of the cover can be calculated by the following approximate equation:

$$\alpha_c \simeq 1 - \tau_a \quad (2.43)$$

The reflectance of the cover can be found from:

$$\rho_c = 1 - (\alpha_c + \tau) \simeq \tau_a - \tau_a \tau_r = \tau_a(1 - \tau_r) \quad (2.44)$$

2.2.5.3 Absorptance of the Absorber

The absorptance for solar radiation of ordinary blackened surfaces is a function of the angle of incidence of the radiation on the surface. However, the angular dependence of solar absorptance of most surfaces used for solar collectors is not available. An example of this dependence, valid for 0° – 90° , is [1]:

$$\begin{aligned} \alpha/\alpha_n = & 1 - 1.5879 \times 10^3 \theta + 2.7314 \times 10^{-4} \theta^2 \\ & - 2.3026 \times 10^{-5} \theta^3 + 9.0244 \times 10^{-7} \theta^4 \\ & - 1.8000 \times 10^{-8} \theta^5 + 1.7734 \times 10^{-10} \theta^6 \\ & - 6.9937 \times 10^{-13} \theta^7 \end{aligned} \quad (2.45)$$

where α_n is the solar absorptance at normal incidence and θ , the angle of incidence, is in degrees.

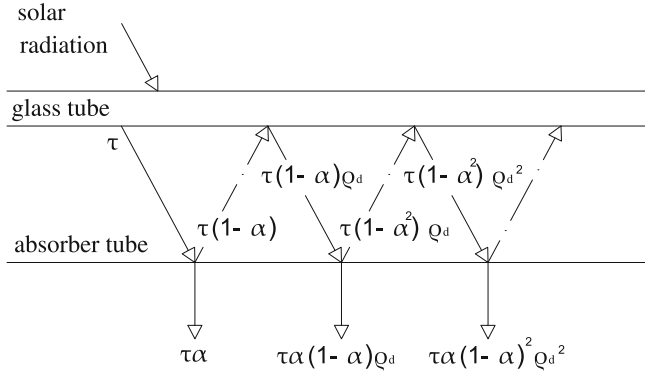


Fig. 2.8 Radiation transfer between the glass and the absorber

2.2.5.4 Transmittance-Absorptance Product

Part of the radiation passing through the cover and incident on the absorber is reflected back to the cover. However, all this radiation is not lost because a portion of it is reflected back to the absorber.

The situation is shown in Fig. 2.8. The fraction $\tau\alpha$ of the incident beam radiation is absorbed by the absorber and the fraction $(1 - \alpha)\tau$ is reflected back to the cover. This radiation, that is assumed to be diffuse and unpolarized, reaches the cover and a fraction $(1 - \alpha)\tau\rho_d$ is reflected back to the absorber. The term ρ_d represents the reflectance of the cover system for diffuse radiation incident from the bottom side and can be evaluated from Eq. (2.44) at an angle of 60° .¹ The multiple reflection of diffuse radiation continues so that the fraction of the incident energy absorbed is

$$(\tau\alpha) = \tau\alpha \sum_{n=0}^{\infty} [(1 - \alpha)\rho_d]^n = \frac{\tau\alpha}{1 - (1 - \alpha)\rho_d} \quad (2.46)$$

The term $(\tau\alpha)$ is usually referred to as the transmittance-absorptance product. It is possible to prove that a reasonable approximation of Eq. (2.46) for most practical solar collectors is [1]:

$$(\tau\alpha) \simeq 1.01\tau\alpha \quad (2.47)$$

¹For a wide range of conditions encountered in solar collector applications, the equivalent angle for beam radiation, i.e. the angle which gives the same reflectance as for diffuse radiation, is essentially 60° [1].

2.3 Thermal Analysis

In this section, we offer a detailed overview of the heat transfer mechanisms participating in a PTC receiver. The definition of thermal efficiency is also given.

2.3.1 Energy Balance of the Receiver

The thermal performance of a PTC can be evaluated by an energy balance that determines the fraction of the incoming radiation delivered as useful energy to the heat transfer fluid (HTF). A number of simplifying assumptions are usually adopted to model such systems [7]:

- Thermal performances are evaluated under steady-state conditions.
- Heat transfer is one-dimensional, i.e. it occurs only through the receiver radial direction. Note that the assumption of one-dimensional energy balance gives reasonable results for short receivers (<100 m), but it is inadequate for longer receivers [8].
- The thermophysical and optical properties of materials are independent of temperature.
- Heat losses through support brackets are neglected.
- The sky can be considered as a blackbody at an equivalent sky temperature for long-wavelength radiation.
- The effects of dust and dirt are negligible.

Figure 2.9 shows the one-dimensional steady-state energy balance for the receiver cross-section of a PTC, while Fig. 2.10 shows the thermal resistance model. When the beam radiation reflected by the concentrator (S_c) strikes the cover, a fraction of solar energy is transmitted to the absorber (τS_c). Only a portion of this energy, S , is effectively conducted through the absorber ($Q_{k,a}$) and transferred to the HTF by convection ($Q_{c,af}$), while a significant portion is lost and transmitted back by convection ($Q_{c,ac}$) and radiation ($Q_{r,ac}$). The energy lost by convective and radiative heat transfers is transmitted by conduction through the cover ($Q_{k,c}$) and, along with the energy absorbed by the cover ($\alpha_c S_c$), is lost to the environment by convection ($Q_{c,ce}$) and radiation ($Q_{r,ce}$).

The system of energy-balance equations is determined by applying the conservation of energy at each surface of the receiver cross-section in Fig. 2.9:

$$\begin{cases} S = Q_{k,a} + Q_{c,ac} + Q_{r,ac} \\ Q_{k,a} = Q_{c,af} = Q_u \\ Q_{c,ac} + Q_{r,ac} = Q_{k,c} \\ Q_{k,c} + \alpha_c S_c = Q_{c,ce} + Q_{r,ce} \end{cases} \quad (2.48)$$

The description of all terms in System (2.48) is provided in Table 2.1.

Fig. 2.9 Energy balance for the receiver cross-section of a PTC. The definition of the symbols is provided in Table 2.1

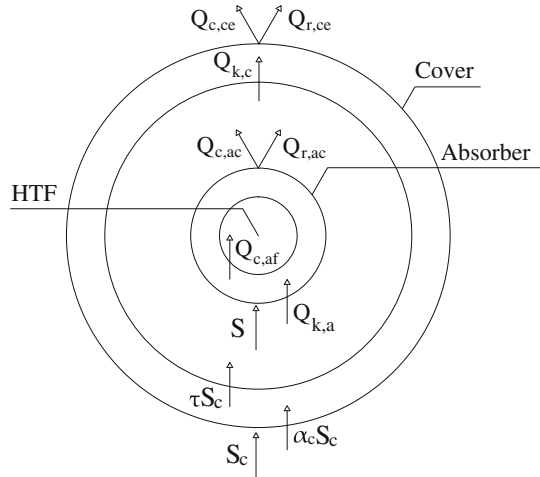
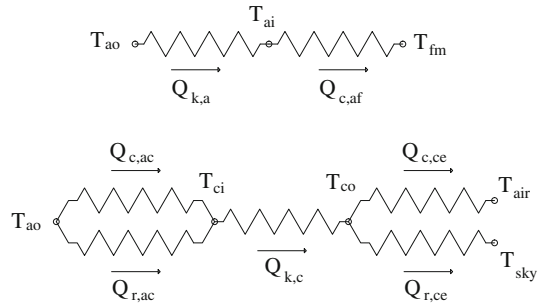


Fig. 2.10 Thermal resistance model of the receiver



The energy-balance system assumes the contribution of the diffuse component of solar radiation to be negligible.² With this assumption, the solar beam radiation reflected by the concentrator to the receiver is:

$$S_c = \rho\gamma G_{bt}A_{ae} \quad (2.49)$$

where

- ρ is the specular reflectance of the concentrator;
- γ is the intercept factor given by Eq. (2.30);
- G_{bt} is the beam radiation measured on the plane of aperture, it can be evaluated with Eqs. (2.14) and (2.15);
- A_{ae} is the effective aperture area defined in Eq. (2.36).

²This assumption is acceptable for all concentrators except for those with low concentration ratio (i.e., for $C = 10$ or below). For systems with low concentration ratio, part of the diffuse radiation will be reflected to the receiver, with the amount depending on the acceptance angle of the concentrator [1].

Table 2.1 Heat fluxes involved in the energy balance of the receiver

Heat flux	Description
S_c	Beam radiation reflected towards the receiver
$\alpha_c S_c$	Beam radiation absorbed by the cover
S	Beam radiation collected by the absorber
$Q_{k,a}$	Conduction through the absorber
$Q_{c,af}$	Convection from the absorber to the fluid
Q_u	Useful heat gain of the fluid
$Q_{c,ac}$	Convection loss from the absorber to the cover
$Q_{r,ac}$	Radiation loss from the absorber to the cover
$Q_{k,c}$	Conduction loss through the cover
$Q_{c,ce}$	Convection loss from the cover to the environment
$Q_{r,ce}$	Radiation loss from the cover to the environment

Thus, the solar beam radiation collected in the absorber is³:

$$S = (\tau\alpha)S_c = (\tau\alpha)\rho\gamma G_{bt}A_{ae} \quad (2.50)$$

where the term $(\tau\alpha)$ is the transmittance-absorptance product defined in Eq. (2.46).

The following sections describe the involved heat fluxes in detail.

2.3.1.1 Conduction Through the Absorber

The conductive heat transfer through the absorber is given by Fourier's law for concentric cylinders:

$$Q_{k,a} = \frac{2\pi\lambda_a L(T_{ao} - T_{ai})}{\ln(D_{ao}/D_{ai})} \quad (2.51)$$

where

- λ_a is the thermal conductivity of the absorber;
- L is the receiver length;
- T_{ao} is the outer absorber temperature;
- T_{ai} is the inner absorber temperature;
- D_{ao} is the outer absorber diameter;
- D_{ai} is the inner absorber diameter.

Note that λ_a is constant and independent of temperature.

³One should also consider the solar beam radiation which falls directly on the absorber tube, but this contribution can be ignored when the concentration ratio is high [9].

2.3.1.2 Internal Convection

The heat transfer between the absorber and the HTF occurs by forced convection and can be expressed by the Newton's law:

$$Q_{c,af} = h_f \pi D_{ai} L (T_{ai} - T_{fm}) \quad (2.52)$$

where T_{fm} is the mean fluid temperature. The convective heat transfer coefficient of the fluid is defined as:

$$h_f = \frac{Nu_f \lambda_f}{D_{ai}} \quad (2.53)$$

where

- Nu_f is the Nusselt number of the HTF;
- λ_f is the thermal conductivity of the HTF.

Note that λ_f is evaluated at the mean fluid temperature.

The Nusselt number depends on the type of flow through the absorber: laminar or transitional/turbulent. For a fluid circulating in a pipe, the flow can be considered laminar when the Reynolds number is lower than 2300. In this condition, the Nusselt number is independent of Reynolds and Prandtl numbers and assumes a constant value equal to 4.36.

On the other hand, the flow of the HTF is within turbulent flow region when $Re_f > 4000$. If $Re_f > 2300$, the Gnielinski's correlation [10] can be used:

$$Nu_f = \frac{(f/8) (Re_f - 1000) Pr_f}{1 + 12.7(f/8)^{1/2} (Pr_f^{2/3} - 1)} \quad (2.54)$$

Equation (2.54) is valid for $0.5 \leq Pr_f \leq 2000$ and $2 \times 10^3 < Re_f < 5 \times 10^6$. The Reynolds and Prandtl numbers must be evaluated at the mean fluid temperature. The friction factor f can be estimated from the Colebrook's iterative formula [11]:

$$\frac{1}{\sqrt{f}} = -2 \log \left(\frac{\xi/D_{ai}}{3.71} + \frac{2.51}{Re_f \sqrt{f}} \right) \quad (2.55)$$

where ξ is the pipe roughness.

2.3.1.3 Convective Loss in the Annulus

The heat lost by convection between the absorber and the cover differs if the annulus is either evacuated or not. In the first case, heat transfer occurs by free-molecular convection; in the second case, heat flux is given by free convection. When the

receiver annulus is under vacuum (i.e., when the pressure is lower than 1 torr), free-molecular convection can be evaluated as [12]:

$$Q_{c,ac} = h_{ann} \pi D_{ao} L (T_{ao} - T_{ci}) \quad (2.56)$$

and

$$h_{ann} = \frac{\lambda_{std}}{D_{ao}/2 \ln(D_{ci}/D_{ao}) + bk(D_{ao}/D_{ci} + 1)} \quad (2.57)$$

$$b = \frac{(2-a)(9\gamma-5)}{2a(\gamma+1)} \quad (2.58)$$

$$k = \frac{2.331 \times 10^{-20} [(T_{ao} + T_{ci})/2 + 273.15]}{p\delta^2} \quad (2.59)$$

where

- h_{ann} is the convective heat transfer coefficient of the annulus gas;
- T_{ci} is the inner cover temperature;
- λ_{std} is the thermal conductivity of the annulus gas at standard temperature and pressure;
- D_{ci} is the inner cover diameter;
- b is the interaction coefficient;
- k is the mean-free path between collisions of a molecule;
- a is the accommodation coefficient;
- γ is the ratio of specific heats for the annulus gas;
- p is the annulus gas pressure;
- δ is the molecular diameter of the annulus gas.

Equation (2.56) can be used when $Ra_{ann} < [D_{ci}/(D_{ci} - D_{ao})]^4$, where Ra_{ann} is the Rayleigh number of the annulus gas. The constants for air as annulus gas are provided in Table 2.2.

If the receiver annulus is not evacuated, heat transfer between the absorber and the cover occurs by free convection:

$$Q_{c,ac} = \frac{2 \pi \lambda_{eff} L}{\ln(D_{ci}/D_{ao})} (T_{ao} - T_{ci}) \quad (2.60)$$

A recommended correlation for the effective conductive coefficient, λ_{eff} , is [13]:

$$\frac{\lambda_{eff}}{\lambda_{ann}} = 0.386 \left(\frac{Pr_{ann}}{0.861 + Pr_{ann}} \right) (F_{cyl} Ra_{ann}) \quad (2.61)$$

Table 2.2 Constants for air as annulus gas at $T_{\text{fm}} = 300^\circ\text{C}$ [14]

$\lambda_{\text{std}} (\text{Wm}^{-1}\text{K}^{-1})$	$k (\text{m})$	$\delta (\text{m})$	b	γ
0.02551	0.8867	3.53×10^{-6}	1.571	1.39

where

- λ_{ann} is the thermal conductivity of air evaluated at mean temperature $(T_{\text{ao}} + T_{\text{ci}})/2$;
- Pr_{ann} is the Prandtl number of air evaluated at mean temperature $(T_{\text{ao}} + T_{\text{ci}})/2$;
- Ra_{ann} is the Rayleigh number of air evaluated at mean temperature $(T_{\text{ao}} + T_{\text{ci}})/2$ and characteristic length $(D_{\text{ci}} - D_{\text{ao}})/2$.

The form factor for concentric cylinders is given by:

$$F_{\text{cyl}} = \frac{[\ln(D_{\text{ci}}/D_{\text{ao}})]^4}{[(D_{\text{ci}} - D_{\text{ao}})/2]^3 (D_{\text{ci}}^{-3/5} + D_{\text{ao}}^{-3/5})^5} \quad (2.62)$$

Equation (2.61) is valid for $0.70 \leq Pr_{\text{ann}} \leq 6000$ and for $10^2 < F_{\text{cyl}} Ra_{\text{ann}} < 10^7$. Note that if $F_{\text{cyl}} Ra_{\text{ann}} < 10^2$, convection is negligible and $\lambda_{\text{eff}} = \lambda_{\text{ann}}$. Finally, λ_{eff} cannot be less than λ_{ann} , so one should set the last equivalence if $\lambda_{\text{eff}} < \lambda_{\text{ann}}$.

2.3.1.4 Radiative Loss in the Annulus

The heat transfer by radiation between the absorber and the cover can be evaluated with the expression:

$$Q_{\text{r,ac}} = \frac{\pi D_{\text{ao}} L \sigma (T_{\text{ao}}^4 - T_{\text{ci}}^4)}{1/\varepsilon_{\text{a}} + (1 - \varepsilon_{\text{c}})(D_{\text{ao}}/D_{\text{ci}})/\varepsilon_{\text{c}}} \quad (2.63)$$

where

- σ is the Stefan–Boltzmann constant ($5.67 \times 10^{-8} \text{ Wm}^{-2} \text{ K}^{-4}$);
- ε_{a} is the emissivity of the absorber in the long-wavelength range;
- ε_{c} is the emissivity of the cover in the long-wavelength range.

In Eq. (2.63), temperatures are in kelvin and emissivities assume constant values.

2.3.1.5 Conductive Loss Through the Cover

The heat transfer mechanism described for the absorber is still valid for the cover. Equation (2.51) can be rewritten as:

$$Q_{\text{k,c}} = \frac{2 \pi \lambda_{\text{c}} L (T_{\text{ci}} - T_{\text{co}})}{\ln(D_{\text{co}}/D_{\text{ci}})} \quad (2.64)$$

where

- λ_c is the thermal conductivity of the cover;
- T_{co} is the outer cover temperature;
- D_{co} is the outer cover diameter.

λ_c is constant and independent of temperature.

2.3.1.6 External Convective Loss

As seen in Sect. 2.3.1.2, the convective heat transfer between the cover and the environment can be expressed through the Newton's law:

$$Q_{c,ce} = h_{air} \pi D_{co} L (T_{co} - T_{air}) \quad (2.65)$$

where T_{air} is the ambient temperature. The convective heat transfer coefficient of air is defined as follows:

$$h_{air} = \frac{Nu_{air} \lambda_{air}}{D_{co}} \quad (2.66)$$

where

- Nu_{air} is the Nusselt number for air;
- λ_{air} is the conductive heat transfer coefficient for air, evaluated at the film temperature $(T_{co} + T_{air})/2$.

Convection will be forced or free depending on the presence or absence of wind. If wind is present, heat transfer occurs by forced convection and the following correlation can be employed [15]:

$$Nu_{air} = 0.3 + \frac{0.62 Re_{air}^{1/2} Pr_{air}^{1/3}}{[1 + (0.4/Pr_{air})^{2/3}]^{1/4}} \left[1 + \left(\frac{Re_{air}}{282000} \right)^{5/8} \right]^{4/5} \quad (2.67)$$

where

- Re_{air} is the Reynolds number for air evaluated at film temperature $(T_{co} + T_{air})/2$ and characteristic length D_{co} ;
- Pr_{air} is the Prandtl number for air evaluated at film temperature $(T_{co} + T_{air})/2$.

The correlation can be used for $Re_{air} Pr_{air} > 0.2$.

If there is no wind, the heat transfer between the cover and the environment will be by free convection. In this case, we propose the correlation [16]:

$$Nu_{air} = \left\{ 0.6 + \frac{0.387 Ra_{air}^{1/6}}{[1 + (0.559/Pr_{air})^{9/16}]^{8/27}} \right\}^2 \quad (2.68)$$

This equation considers a long isothermal horizontal cylinder and it can be adopted for $10^5 < Ra_{\text{air}} < 10^{12}$. Considerations made for Reynolds and Prandtl numbers in Eq. (2.67) are still valid.

2.3.1.7 External Radiative Loss

The radiative heat transfer between the cover and the environment is caused by the temperature difference between the outer cover surface and the sky. This condition is approximated by considering a small convex gray object (the cover) in a large blackbody cavity (the sky). Therefore, the net exchanged radiation is:

$$Q_{r,ce} = \varepsilon_c \pi D_{co} L \sigma (T_{co}^4 - T_{sky}^4) \quad (2.69)$$

Temperatures are in kelvin and emissivities are constant.

The sky temperature T_{sky} can be related to the dry bulb temperature T_{air} and the dew point ambient temperature T_{dp} as follows [17]:

$$T_{sky} = \varepsilon_{sky}^{1/4} T_{air} \quad (2.70)$$

where the sky emissivity is given by

$$\varepsilon_{sky} = 0.711 + 0.56 \left(\frac{T_{dp}}{100} \right) + 0.73 \left(\frac{T_{dp}}{100} \right)^2 \quad (2.71)$$

2.3.2 Thermal Efficiency

The thermal efficiency of a PTC is defined as the ratio of the useful heat gain of the HTF, Q_u , to the solar energy intercepted by the collector aperture area, S_a , and is given by:

$$\eta = \frac{Q_u}{S_a} = \frac{\dot{m} c_p (T_{fo} - T_{fi})}{G_{bt} A_a} \quad (2.72)$$

where:

- \dot{m} is the mass flow rate of the HTF;
- c_p is the specific heat at constant pressure of the HTF;
- T_{fo} is the outlet fluid temperature;
- T_{fi} is the inlet fluid temperature;
- G_{bt} is the beam radiation measured on the plane of aperture (it must be properly evaluated by using Eqs. (2.14) and (2.15));
- A_a is the collector aperture area.

An energy balance alternative to System (2.48) can be extended to a control volume containing only the absorber. For a PTC of aperture area A_a , the energy balance on the cylindrical absorber yields:

$$S = Q_u + Q_l + \frac{dE_c}{dt} \quad (2.73)$$

where

- S is the solar beam radiation collected in the absorber tube after reflection, defined by Eq. (2.50);
- Q_u is the rate of useful heat gain;
- Q_l is the rate of heat loss from the absorber;
- dE_c/dt is the rate of internal energy storage in the collector.

Equation (2.73) can be rewritten in terms of an overall loss coefficient, U_L , by considering the expression:

$$Q_l = U_L A_r (T_r - T_{air}) \quad (2.74)$$

where

- A_r is the area of the absorber surface (equal to $\pi D_{ao}L$);
- T_r is the average temperature of the absorber surface;
- T_{air} is the ambient temperature.

Substituting Eq. (2.74) in (2.73), operating in steady state conditions ($dE_c/dt = 0$) and rearranging terms, one gets⁴:

$$Q_u = (\tau\alpha)\rho\gamma G_{bt}A_{ae} - U_L A_r (T_r - T_{air}) \quad (2.75)$$

The problem with this equation is that the average temperature of the absorber surface, T_r , is difficult to calculate or measure since it is a function of the collector design, the incident solar radiation and the entering fluid conditions. However, one can use T_{fi} , the inlet fluid temperature, instead of T_r , by introducing a heat removal factor F_R :

$$Q_u = F_R [(\tau\alpha)\rho\gamma G_{bt}A_{ae} - U_L A_r (T_{fi} - T_{air})] \quad (2.76)$$

where

$$F_R = \frac{\dot{m}c_p}{A_r U_L} \left[1 - \exp\left(-\frac{A_r U_L F'}{\dot{m}c_p}\right) \right] \quad (2.77)$$

⁴Some authors define an effective transmittance-absorptance product which accounts for the reduced thermal losses due to absorption of solar radiation by the cover. However, this effect has been already considered in the energy balance of Eq. (2.48), thus it will be not reconsidered here.

The heat removal factor is an important design parameter since it is a measure of the thermal resistance encountered by the absorbed radiation in reaching the HTF. From Eq. (2.76), it is possible to define F_R as the ratio of the useful heat gain of the fluid to the gain which would occur if the absorber were at temperature T_{fi} everywhere. Note that F_R can range between 0 and 1.

The term F' is the collector efficiency factor and represents the ratio of the useful heat gain of the fluid to the gain which would occur if the whole absorber were at the local fluid temperature. It is given by:

$$F' = \frac{1/U_L}{1/U_L + D_{ao}/(h_f D_{ai}) + D_{ao} \ln (D_{ao}/D_{ai})/(2\lambda_a)} \quad (2.78)$$

where

- h_f is the convective heat transfer coefficient of the fluid defined in Eq. (2.53);
- λ_a is the thermal conductivity of the absorber.

Equation (2.76) is the Hottel–Whillier–Bliss equation adapted for PTCs. Dividing this equation by the solar energy intercepted by the collector aperture area, S_a , one gets:

$$\eta = \frac{Q_u}{S_a} = F_R \left[\eta_o - \frac{U_L}{C} \left(\frac{T_{fi} - T_{air}}{G_{bt}} \right) \right] \quad (2.79)$$

where η_o is the optical efficiency of the PTC, the ratio of solar energy collected by the absorber to that intercepted by the concentrator. The optical efficiency can be written as:

$$\eta_o = (\tau\alpha)\rho\gamma(1 - A_f) \quad (2.80)$$

Equation (2.79) is an alternative form of Eq. (2.72) and allows to determine the thermal efficiency of a PTC as a function of the term $(T_{fi} - T_{air})/G_{bt}$.

As a general comment, it is worth noting that the concentration ratio has a relevant role in reducing the thermal losses of a PTC: from Eq. (2.79), it is evident that the greater is the concentration ratio, the higher is the efficiency. Optical efficiency also assumes a decisive role.

References

1. Duffie JA, Beckman WA (2013) Solar engineering of thermal processes, 4th edn. Wiley, Hoboken
2. Kalogirou SA (2014) Solar energy engineering: processes and systems, 2nd edn. Elsevier, Oxford
3. Rabl A (1976) Comparison of solar concentrators. Sol Energy 18(2):93–111
4. Treadwell GW (1976) Design considerations for parabolic-cylindrical solar collectors. In: Sharing the sun: solar technology in the seventies, vol 2, pp 235–252

5. Guven HM, Bannerot RB (1986) Derivation of universal error parameters for comprehensive optical analysis of parabolic troughs. *J Sol Energy Eng* 108:275–281
6. Jeter SM, Jarrar DI, Moustafa SA (1983) Geometrical effects on the performance of trough collectors. *Sol Energy* 30:109–113
7. Coccia G, Latini G, Sotte M (2012) Mathematical modeling of a prototype of parabolic trough solar collector. *J Renew Sustain Energy* 4(2):023110
8. Forristall R (2003) Heat transfer analysis and modeling of a parabolic trough solar receiver implemented in engineering equation solver. NREL, Golden
9. Sukhatme SP, Nayak JK (2008) *Solar energy: principles of thermal collection and storage*. Tata McGraw-Hill Publishing Company, New Delhi
10. Gnielinski V (1975) New equations for heat and mass transfer in the turbulent flow in pipes and channels. NASA, STI/Recon technical report A, vol 41, pp 8–16
11. Colebrook CF (1939) Turbulent flow in pipes, with particular reference to the transition region between the smooth and rough pipe laws. *J ICE* 11:133–156
12. Ratzel A, Hickox C, Gartling D (1979) Techniques for reducing thermal conduction and natural convection heat losses in annular receiver geometries. *J Heat Trans-T ASME* 101(1):108–113
13. Hollands KGT, Raithby GD, Lonicek L (1975) Correlation equations for free convection heat transfer in horizontal layers of air and water. *Int J Heat Mass Transf* 18(7):879–884
14. Marshal N (1976) *Gas encyclopedia*. Elsevier, New York
15. Churchill SW, Bernstein M (1977) A correlating equation for forced convection from gases and liquids to a circular cylinder in crossflow. *J Heat Trans-T ASME* 99:300–306
16. Churchill SW, Chu HHS (1975) Correlating equations for laminar and turbulent free convection from a horizontal cylinder. *Int J Heat Mass Transf* 18(9):1049–1053
17. Martin M, Berdahl P (1984) Characteristics of infrared sky radiation in the United States. *Sol Energy* 33(3):321–336

Parabolic Trough Collector Prototypes for
Low-Temperature Process Heat

Coccia, G.; Di Nicola, G.; Hidalgo, A.

2016, XIX, 80 p. 29 illus., 19 illus. in color., Softcover

ISBN: 978-3-319-27082-1